

DESY 04-040
hep-ph/0405232
May 2004

ISSN 0418-9833

Two-loop electroweak correction of $\mathcal{O}(G_F M_t^2)$ to the Higgs-boson decay into photons

Frank Fugel, Bernd A. Kniehl, Matthias Steinhauser

II. Institut für Theoretische Physik, Universität Hamburg,
Luruper Chaussee 149, 22761 Hamburg, Germany

Abstract

We compute the dominant two-loop electroweak correction, of $\mathcal{O}(G_F M_t^2)$, to the partial width of the decay of an intermediate-mass Higgs boson into a pair of photons. We use the asymptotic-expansion technique in order to extract the leading dependence on the top-quark mass plus four expansion terms that describe the dependence on the W - and Higgs-boson masses. This correction reduces the Born result by approximately 2.5%. As a by-product of our analysis, we also recover the $\mathcal{O}(G_F M_t^2)$ correction to the partial width of the Higgs-boson decay to two gluon jets.

PACS numbers: 12.15.Ji, 12.15.Lk, 14.80.Bn

1 Introduction

Among the main tasks of the current experiments at the Fermilab Tevatron and the future experiments at the CERN Large Hadron Collider (LHC) is the search for the Higgs boson, which is the only missing particle in the standard model (SM). The electroweak precision data mainly collected at CERN LEP and SLAC SLC in combination with the direct top-quark mass measurement at the Tevatron favour a light Higgs boson with mass $M_H = 113^{+62}_{-42}$ GeV with an upper bound of about 237 GeV at the 95% confidence level [1]. The allowed mass range is compatible with the so-called intermediate mass range, defined by $M_W \leq M_H \leq 2M_W$. In this mass range, the decay into two photons represents one of the most useful detection modes at hadron colliders.

Since there is no direct coupling of the Higgs boson to photons, the process $H \rightarrow \gamma\gamma$ is loop-induced. In the limit of vanishing bottom-quark mass, one distinguishes at lowest order the contributions from virtual top quarks and W bosons, where, in covariant gauge, the latter are accompanied by charged Goldstone bosons (ϕ) and Faddeev-Popov ghosts (u). Some sample Feynman diagrams are depicted in Fig. 1. The corresponding contributions have been evaluated for the first time in Ref. [2] (for reviews, see also Ref. [3]). QCD corrections, which only affect the top-quark diagrams are known at the two- [4] and three-loop [5] orders. Recently, also the two-loop electroweak correction induced by light-fermion loops has been evaluated [6]. In this paper, we compute the two-loop electroweak correction that is enhanced by $G_F M_t^2$. For this purpose, we consider the (formal) hierarchy $M_t^2 \gg (2M_W)^2 \gg M_H^2$ and apply the method of asymptotic expansion [7], which allows us to also evaluate four expansion terms in the ratio $\tau_W = M_H^2/(2M_W)^2$ aside from the leading term in M_t^2 .

Due to electromagnetic gauge invariance, the amputated transition-matrix element of $H \rightarrow \gamma\gamma$ possesses the structure

$$\mathcal{T}^{\mu\nu} = (q_1 \cdot q_2 g^{\mu\nu} - q_1^\nu q_2^\mu) \mathcal{A}, \quad (1)$$

where μ and ν are the Lorentz indices of the external photons with four-momenta q_1 and q_2 , respectively. Thus, the decay rate of the Higgs boson into two photons is given by

$$\Gamma(H \rightarrow \gamma\gamma) = \frac{M_H^3}{64\pi} |\mathcal{A}|^2. \quad (2)$$

The form factor \mathcal{A} is evaluated in perturbation theory as

$$\mathcal{A} = \mathcal{A}_t^{(0)} + \mathcal{A}_W^{(0)} + \mathcal{A}_{tW}^{(1)} + \dots, \quad (3)$$

where $\mathcal{A}_t^{(0)}$ and $\mathcal{A}_W^{(0)}$ denote the one-loop contributions induced by virtual top quarks and W bosons, respectively, $\mathcal{A}_{tW}^{(1)}$ stands for the two-loop electroweak correction involving virtual top quarks, and the ellipsis represents the residual one- and two-loop contributions as well as all contributions involving more than two loops.

In the practical calculation, it is convenient to project out the scalar amplitudes that multiply the basic Lorentz tensors $g^{\mu\nu}$, $q_1^\mu q_2^\nu$, and $q_1^\nu q_2^\mu$. The corresponding projectors

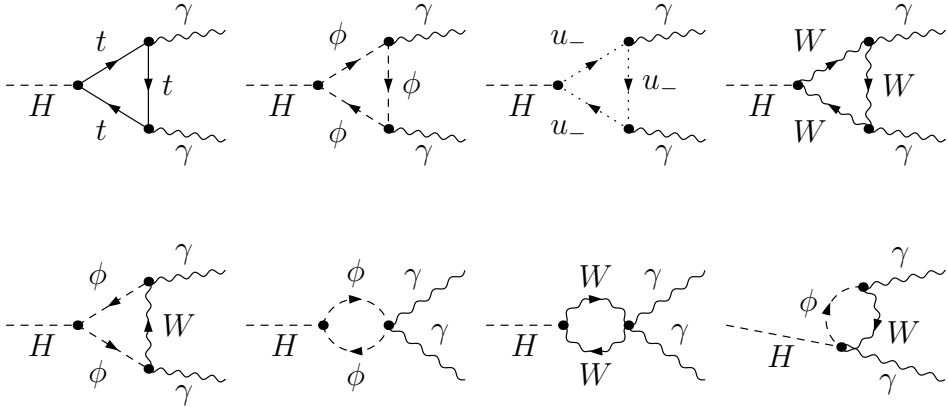


Figure 1: Sample Feynman diagrams contributing in leading order to the process $H \rightarrow \gamma\gamma$.

can be obtained by in turn contracting $\mathcal{T}^{\mu\nu}$ with these Lorentz tensors and solving the resulting system of linear equations. We separately project out the coefficients of the tensors $q_1 \cdot q_2 g^{\mu\nu}$ and $q_1^\nu q_2^\mu$, and thus have a strong check on our calculation. Furthermore, we adopt a general R_ξ gauge in our calculation and verify that the gauge parameter drops out in the final result. For simplicity, the element V_{tb} of the Cabibbo-Kobayashi-Maskawa quark mixing matrix is set to unity, so that the quarks of the third fermion generation decouple from those of the first two, which they actually do to very good approximation [8].

Our paper is organized as follows. In Section 2, we illustrate the usefulness of the asymptotic-expansion technique by redoing the one-loop calculation. In Section 3, we discuss the two-loop calculation. Section 4 contains the discussion of the numerical results. We conclude with a summary in Section 5.

2 One-loop results and counterterm contribution

The application of the asymptotic-expansion technique to the one-loop diagrams, some of which are shown in Fig. 1, leads to a naive Taylor expansion in the external momenta q_1 and q_2 . Nevertheless, we use already here a completely automated set-up, which consists in the successive use of the computer programs **QGRAF** [9], **q2e** [10], **exp** [11], and **MATAD** [12]. First, **QGRAF** is used to generate the Feynman diagrams. Its output is then rewritten by **q2e** to be understandable by **exp**. In the two-loop case, the latter performs the asymptotic expansion and generates the relevant subdiagrams according to the rules of the so-called hard-mass procedure [7]. **Form** [13] files are generated, which can be read by **MATAD** [12], which performs the very calculation of the diagrams.

The analytic expression for the Born result can be found in Refs. [2, 14]. For completeness, we list it here in closed form and as an expansion for $(2M_W)^2 \gg M_H^2$, which

we reproduce. One has

$$\begin{aligned}\mathcal{A}_t^{(0)} &= \hat{\mathcal{A}} N_c Q_t^2 \left\{ \frac{1}{\tau_t} \left[1 + \left(1 - \frac{1}{\tau_t} \right) \arcsin^2 \sqrt{\tau_t} \right] \right\} \\ &= \hat{\mathcal{A}} N_c Q_t^2 \left(\frac{2}{3} + \frac{7}{45} \tau_t + \frac{4}{63} \tau_t^2 + \frac{52}{1575} \tau_t^3 + \frac{1024}{51975} \tau_t^4 + \frac{2432}{189189} \tau_t^5 + \dots \right),\end{aligned}\quad (4)$$

$$\begin{aligned}\mathcal{A}_W^{(0)} &= \hat{\mathcal{A}} \left\{ -\frac{1}{2} \left[2 + \frac{3}{\tau_W} + \frac{3}{\tau_W} \left(2 - \frac{1}{\tau_W} \right) \arcsin^2 \sqrt{\tau_W} \right] \right\} \\ &= \hat{\mathcal{A}} \left(-\frac{7}{2} - \frac{11}{15} \tau_W - \frac{38}{105} \tau_W^2 - \frac{116}{525} \tau_W^3 - \frac{2624}{17325} \tau_W^4 - \frac{640}{5733} \tau_W^5 + \dots \right),\end{aligned}\quad (5)$$

where $\hat{\mathcal{A}} = 2^{1/4} G_F^{1/2} (\alpha/\pi)$, $\tau_t = M_H^2/(2M_t)^2$, and τ_W is defined in Section 1. Here, α is Sommerfeld's fine-structure constant, G_F is Fermi's constant, $N_c = 3$ is the number of quark colours, and $Q_t = 2/3$ is the electric charge of the top quark in units of the positron charge. The Higgs-boson mass entering the expansion parameters τ_t and τ_W partly arises from the couplings involving one Higgs and two Goldstone bosons, but also from the expansion in the external momenta due to the kinematic relation $(q_1 + q_2)^2 = M_H^2$.

We wish to note that the result for the process $H \rightarrow gg$ is simply obtained by setting $\mathcal{A}_W^{(0)} = 0$ and performing the substitution $\alpha N_c Q_t^2 \rightarrow \alpha_s \sqrt{2}$, where α_s is the strong-coupling constant.

In the remainder of this section, let us discuss the counterterm contributions needed for our two-loop analysis. We adopt the on-mass-shell scheme and regularize the ultra-violet divergences by means of dimensional regularization, with $D = 4 - 2\epsilon$ space-time dimensions and 't Hooft mass scale μ . We use the anti-commuting definition of γ_5 .

As will become clearer in the next section, it is important to treat the tadpole contributions properly in our calculation. For this reason, in the following, we list the corresponding contributions separately and mark them by the superscript "tad". Inspection of the one-loop diagrams reveals that, to $\mathcal{O}(G_F M_t^2)$, we have to renormalize the Higgs-boson wave function and mass, the W -boson mass, and the top-quark mass. The corresponding counterterms are defined through

$$\begin{aligned}H^0 &= \sqrt{Z_H} H = \left(1 + \frac{1}{2} \delta Z_H \right) H, \\ (M_H^0)^2 &= M_H^2 + \delta M_H^2 + \delta M_H^{2,\text{tad}}, \\ (M_W^0)^2 &= M_W^2 + \delta M_W^2 + \delta M_W^{2,\text{tad}}, \\ M_t^0 &= M_t + \delta M_t + \delta M_t^{\text{tad}}.\end{aligned}\quad (6)$$

Note that δZ_H is obtained from the derivative of the Higgs-boson self-energy and thus has no tadpole contribution. The mass counterterms are obtained from the corresponding two-point functions, where only the M_t -enhanced contributions have to be considered. Up to and including quadratic terms in M_t , we have

$$\delta Z_H = -2N_c x_t \left(\Delta - \ln \frac{M_t^2}{\mu^2} - \frac{2}{3} \right),$$

$$\begin{aligned}
\frac{\delta M_H^2}{M_H^2} &= N_c x_t \left[-12 \frac{M_t^2}{M_H^2} \left(\Delta - \ln \frac{M_t^2}{\mu^2} + \frac{1}{3} \right) + 2 \left(\Delta - \ln \frac{M_t^2}{\mu^2} - \frac{2}{3} \right) \right], \\
\frac{\delta M_H^{2,tad}}{M_H^2} &= 12 N_c x_t \frac{M_t^2}{M_H^2} \left(\Delta - \ln \frac{M_t^2}{\mu^2} + 1 \right), \\
\frac{\delta M_W^2}{M_W^2} &= -2 N_c x_t \left(\Delta - \ln \frac{M_t^2}{\mu^2} + \frac{1}{2} \right), \\
\frac{\delta M_W^{2,tad}}{M_W^2} &= 8 N_c x_t \frac{M_t^2}{M_H^2} \left(\Delta - \ln \frac{M_t^2}{\mu^2} + 1 \right), \\
\frac{\delta M_t}{M_t} &= \frac{3}{2} x_t \left(\Delta - \ln \frac{M_t^2}{\mu^2} + \frac{8}{3} \right), \\
\frac{\delta M_t^{tad}}{M_t} &= 4 N_c x_t \frac{M_t^2}{M_H^2} \left(\Delta - \ln \frac{M_t^2}{\mu^2} + 1 \right), \tag{7}
\end{aligned}$$

with $x_t = G_F M_t^2 / (8\pi^2 \sqrt{2})$ and $\Delta = 1/\epsilon - \gamma_E + \ln(4\pi)$, where γ_E is Euler's constant. The W -boson mass renormalization is needed for the W , ϕ , and u propagators, where M_W enters as a parameter. Furthermore, also the $HW^\pm W^\mp$, $H\phi^\pm W^\mp$, $\phi^\pm W^\mp \gamma$, and $H\phi^\pm W^\mp \gamma$ vertices contain M_W . The only vertex involving M_H is $H\phi^\pm \phi^\mp$, which induces two-loop contributions via δM_H . Finally, M_t occurs in the top-quark propagator and in the $Ht\bar{t}$ vertex.

The wave function renormalization and the renormalization of a factor $1/M_W$ is common to all one-loop diagrams. This allows for the definition of a universal factor [15], which is finite in our calculation. It is given by

$$\begin{aligned}
\delta_u &= \frac{1}{2} \left(\delta Z_H - \frac{\delta M_W^2}{M_W^2} \right) \\
&= \frac{7}{6} N_c x_t. \tag{8}
\end{aligned}$$

3 Two-loop results

The contributions of $\mathcal{O}(G_F M_t^2)$ are obtained by considering all two-loop electroweak diagrams involving a virtual top quark. This includes also the tadpole diagrams with a closed top-quark loop, which are proportional to M_t^4 . For arbitrary gauge parameter, this leads us to consider a total of $\mathcal{O}(1000)$ diagrams. Some of them are depicted in Fig. 2. These diagrams naturally split into two classes. The first class consists of those diagrams where a neutral boson, i.e. a Higgs boson or a neutral Goldstone boson (χ), is added to the one-loop top-quark diagrams. The exchange of a Z boson does not produce quadratic contributions in M_t . The application of the asymptotic-expansion technique to these diagrams leads to a simple Taylor expansion in the external momenta.

This is different for the second class of diagrams, which, next to the top quark, also contain a W or ϕ boson and, as a consequence, also the bottom quark, which we take

to be massless throughout the calculation. Due to the presence of cuts through light-particle lines, the asymptotic-expansion technique applied to these diagrams also yields nontrivial terms, as is exemplified in Fig. 3. The first contribution on the right-hand side of the equation in Fig. 3 symbolizes the naive Taylor expansion in the external momenta. In the second contribution, the subdiagram to the right of the star has to be expanded in its external momenta, which also includes the loop momentum of the co-subgraph to the left of the star. The result of the expansion is inserted as an effective vertex, and the remaining integration over the second loop-momentum is performed after a further expansion in q_1 and q_2 . The latter is allowed, since we work in the limit $(2M_W)^2 \gg M_H^2$. We wish to mention that such contributions develop M_t^4 terms, which cancel in the final result only in combination with the M_t^4 terms from the counterterms of Eq. (7) and the genuine two-loop tadpole diagrams. For this reason, it is crucial to include the latter in our calculation. As a further comment, we note that, unlike the example of Fig. 3, it can also happen that the co-subgraph only involves massless bottom quarks, and no expansion in the external momenta is allowed. In our calculation, the contributions from such co-subgraphs vanish.

As already mentioned above, we use in our calculation a general gauge parameter ξ_W related to the W boson and verify that our final result is independent of ξ_W . We do this in the limit of large and small values of ξ_W . To this end, we apply the asymptotic-expansion technique in the following four limiting cases

- (i) $M_t^2 \gg M_W^2 = \xi_W M_W^2 \gg M_H^2$,
- (ii) $M_t^2 \gg M_W^2 \gg \xi_W M_W^2 \gg M_H^2$,
- (iii) $M_t^2 \gg \xi_W M_W^2 \gg M_W^2 \gg M_H^2$,
- (iv) $\xi_W M_W^2 \gg M_t^2 \gg M_W^2 \gg M_H^2$,

(9)

where the inequality $M_W^2 \gg M_H^2$ has to be understood in a formal sense, as, in practice, one has $(2M_W)^2 \gg M_H^2$. The result we obtain by asymptotic expansion is an expansion of the exact result for the $\mathcal{O}(G_F M_t^2)$ contribution in powers of τ_W . In case (i), where $\xi_W = 1$, which corresponds to 't Hooft-Feynman gauge, we are able to evaluate the first five terms of this expansion. In cases (ii)–(iv), we compute the first two expansion terms and find agreement with the result obtained for $\xi_W = 1$.

Our final result for $\mathcal{A}_{tW}^{(1)}$ emerges as the sum

$$\mathcal{A}_{tW}^{(1)} = \mathcal{A}_u^{(1)} + \mathcal{A}_{H,\chi}^{(1)} + \mathcal{A}_{W,\phi}^{(1)}, \quad (10)$$

where $\mathcal{A}_u^{(1)}$ is the universal contribution induced by the one-loop term δ_u of Eq. (8), $\mathcal{A}_{H,\chi}^{(1)}$ is the two-loop contribution involving virtual H and χ bosons, and $\mathcal{A}_{W,\phi}^{(1)}$ the remaining two-loop contribution involving virtual W and ϕ bosons. In $\mathcal{A}_{H,\chi}^{(1)}$ and $\mathcal{A}_{W,\phi}^{(1)}$, also the corresponding counterterm and tadpole contributions are included. For the individual pieces, we find

$$\mathcal{A}_u^{(1)} = \hat{\mathcal{A}} N_c x_t \left(-\frac{329}{108} - \frac{77}{90} \tau_W - \frac{19}{45} \tau_W^2 - \frac{58}{225} \tau_W^3 - \frac{1312}{7425} \tau_W^4 + \dots \right),$$

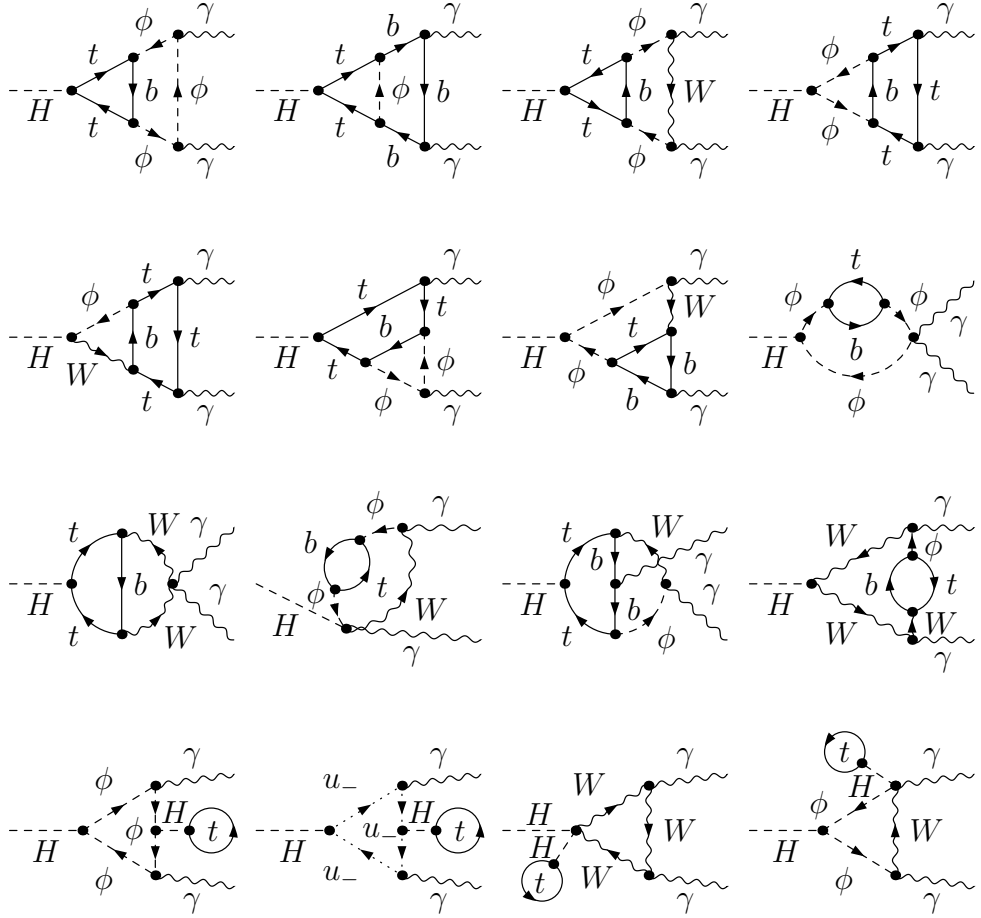


Figure 2: Sample Feynman diagrams contributing at the two-loop electroweak order to the process $H \rightarrow \gamma\gamma$.

$$\begin{aligned} \mathcal{A}_{H,\chi}^{(1)} &= \hat{\mathcal{A}} N_c x_t \left(-\frac{8}{27} \right), \\ \mathcal{A}_{W,\phi}^{(1)} &= \hat{\mathcal{A}} N_c x_t \left(\frac{182}{27} + \frac{22}{15} \tau_W + \frac{76}{105} \tau_W^2 + \frac{232}{525} \tau_W^3 + \frac{5248}{17325} \tau_W^4 + \dots \right), \end{aligned} \quad (11)$$

where $\hat{\mathcal{A}}$ is defined below Eq. (5) and the ellipses indicate terms of $\mathcal{O}(\tau_W^5)$. Notice that the leading $\mathcal{O}(G_F M_t^2)$ term of $\mathcal{A}_{H,\chi}^{(1)}$ is not accompanied by an expansion in τ_W , since the contributing diagrams do not involve virtual W or ϕ bosons. On the other hand, detailed inspection reveals that there is also no expansion in the parameter $M_H^2/(2M_Z)^2$, contrary to what might be expected at first sight. Inserting Eq. (11) into Eq. (10), we obtain our

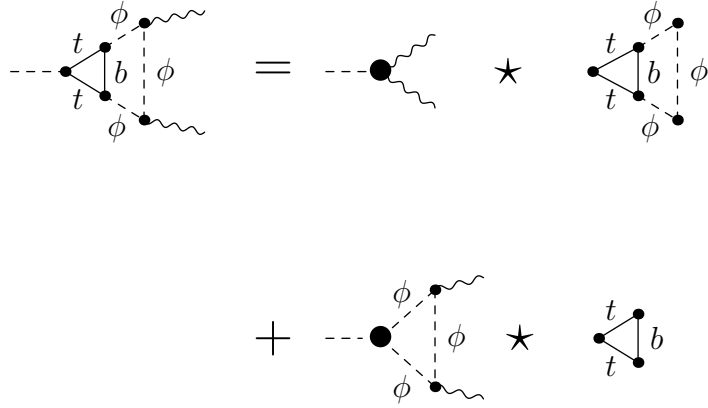


Figure 3: Diagrammatic asymptotic expansion of a Feynman diagram that produces M_t^4 terms.

final result

$$\mathcal{A}_{tW}^{(1)} = \hat{\mathcal{A}} N_c x_t \left(\frac{367}{108} + \frac{11}{18} \tau_W + \frac{19}{63} \tau_W^2 + \frac{58}{315} \tau_W^3 + \frac{1312}{10395} \tau_W^4 + \dots \right). \quad (12)$$

The correction of $\mathcal{O}(G_F M_t^2)$ to $\Gamma(H \rightarrow \gamma\gamma)$ was also considered in Ref. [16]. The expression found in that reference disagrees with our result. One reason is probably that the authors of Ref. [16] only considered virtual ϕ bosons, but disregarded virtual W -bosons. However, our calculation shows that both types of charged bosons have to be taken into account at the same time in order to arrive at an ultraviolet-finite and gauge-parameter-independent result. In Ref. [17], the dominant two-loop electroweak corrections to the Higgs-boson couplings to pairs of gauge bosons and light fermions induced by a sequential isodoublet of ultraheavy quarks (A, B) were investigated by means of a low-energy theorem [14, 18]. In that paper, also a result for the $\mathcal{O}(G_F M_t^2)$ correction to $\Gamma(H \rightarrow \gamma\gamma)$ is presented, which is obtained by sending the mass of the fourth-generation down quark (M_B) to zero at the end of the calculation, which is performed assuming that $M_B \gg M_W$. This result also deviates from the one obtained above. Detailed inspection reveals that this difference may be attributed to the interchange of limits performed in Ref. [17], which is not justified in the case under consideration, although such a procedure is known to lead to correct results in simpler examples. In fact, reanalyzing the limiting case $M_A \gg M_B \gg M_W$ using the asymptotic-expansion technique, we are able to reproduce the terms of Eqs. (48)–(54) in Ref. [17] that survive in this limit and, at the same time, to identify contributions that do not occur if $M_B = 0$ is imposed at the outset of the calculation.

For completeness, we also specify our corresponding result for $\Gamma(H \rightarrow gg)$. Its evaluation is significantly simpler, since, at one loop, only the top-quark diagrams contribute.

Consequently, to obtain the leading two-loop correction proportional to $G_F M_t^2$, we only have to consider the exchange of H , χ , and ϕ bosons. This only requires a naive Taylor expansion in q_1 and q_2 . We obtain

$$\mathcal{A}_{gg}^{(1)} = \hat{\mathcal{A}}_{gg} x_t \left(\frac{1}{3} \right), \quad (13)$$

with $\hat{\mathcal{A}}_{gg} = 2^{3/4} G_F^{1/2} (\alpha_s / \pi)$. This result is in agreement with Ref. [19], where a low-energy theorem [14, 18] was used.

4 Numerical results

We are now in a position to present our numerical results and to assess the convergence properties of our expansions in τ_t and τ_W . We use the following numerical values for our input parameters [8]: $G_F = 1.16639 \times 10^{-5}$ GeV $^{-2}$, $M_W = 80.423$ GeV, and $M_t = 174.3$ GeV.

We first consider the one-loop amplitudes $\mathcal{A}_t^{(0)}$ and $\mathcal{A}_W^{(0)}$ induced by virtual top quarks and W bosons, respectively, for which exact results are available. They are shown in Figs. 4 and 5 as functions of τ_t and τ_W , respectively. The solid curves indicate the exact results, while the dashed curves represent the sequences of approximations that are obtained by successively including higher powers of τ_t and τ_W , respectively, in the expansions. The vertical lines encompass the intermediate-mass range of the Higgs boson, $M_W \leq M_H \leq 2M_W$. In Fig. 5, the second vertical line coincides with the right edge of the frame. From Fig. 4, we observe that the approximation consisting of the first three terms of the expansion in τ_t is practically indistinguishable from the exact result up to $\tau_t \approx 0.25$. The same is true for the sum of the first five expansion terms up to $\tau_t \approx 0.5$, which corresponds to $M_H \approx 245$ GeV. In the case of $\mathcal{A}_W^{(0)}$, the convergence is slightly worse, since $M_H = 2M_W$ corresponds to $\tau_W = 1$ and the exact result behaves like $\sqrt{1 - \tau_W}$ in this limit. Nevertheless, for $M_H = 120$ GeV, 140 GeV, and $2M_W$, the approximation by five expansion terms deviates from the exact result by as little as 0.3%, 1.6%, and 19.9%, respectively.

Having demonstrated the fast convergence of the expansions in τ_t and τ_W of the one-loop amplitudes $\mathcal{A}_t^{(0)}$ and $\mathcal{A}_W^{(0)}$, respectively, we now proceed to the two-loop electroweak amplitude $\mathcal{A}_{tW}^{(1)}$, for which we found the leading $\mathcal{O}(G_F M_t^2)$ term together with its sub-leading mass corrections through $\mathcal{O}(\tau_W^4)$. This corresponds to a first approximation and four improvements, which are visualized by the five dashed curves in Fig. 6. As in Fig. 5, the dotted vertical line and the right edge of the frame enclose the intermediate-mass range of the Higgs boson. We again observe rapid convergence. The goodness of our best approximation may be assessed by considering its relative deviation from the second best one. For $M_H = 120$ GeV, 140 GeV, and $2M_W$, this amounts to 0.3%, 1.0%, and 2.8%, respectively. The situation is very similar to the one in Fig. 5. In fact, the corresponding figures for $\mathcal{A}_W^{(0)}$ are 0.4%, 1.1%, and 3.1%. We thus expect that the goodness of the approximation of $\mathcal{A}_{tW}^{(1)}$ by the expansion through $\mathcal{O}(\tau_W^4)$ is comparable to the case of $\mathcal{A}_W^{(0)}$.

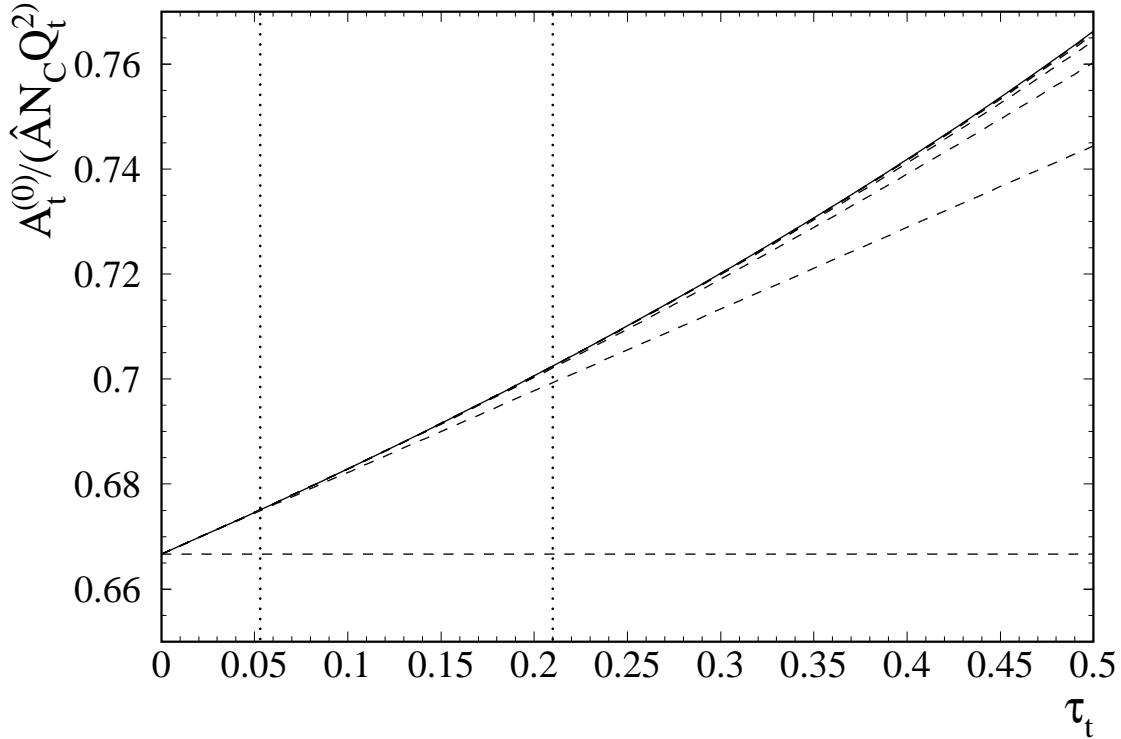


Figure 4: Top-quark-induced one-loop amplitude $\mathcal{A}_t^{(0)}$ normalized to $\hat{A}N_cQ_t^2$ as a function of τ_t . The solid curve indicates the exact result, while the dashed curves represent the sequence of approximations that are obtained by successively including higher powers of τ_t in the expansion. The dotted vertical lines encompass the intermediate-mass range of the Higgs boson.

For the comparison with future measurements of $\Gamma(H \rightarrow \gamma\gamma)$, all known corrections have to be included in Eq. (3). In this connection, it is interesting to compare the size of the new $\mathcal{O}(G_F M_t^2)$ electroweak correction with the well-known $\mathcal{O}(\alpha_s)$ QCD one [4]. This is done in Fig. (7), where the respective corrections to $\Gamma(H \rightarrow \gamma\gamma)$ are displayed as functions of M_H . As in Figs. 5 and 6, the dotted vertical line and the right edge of the frame margin the intermediate-mass range of the Higgs boson. We observe that, within the latter, the $\mathcal{O}(G_F M_t^2)$ correction slightly exceeds the $\mathcal{O}(\alpha_s)$ one in magnitude, a rather surprising finding. Due to the sign difference, the two corrections practically compensate each other. The two-loop electroweak correction induced by light-fermion loops, which has become available recently [6], is also negative, but has a slightly smaller size than the $\mathcal{O}(G_F M_t^2)$ correction.

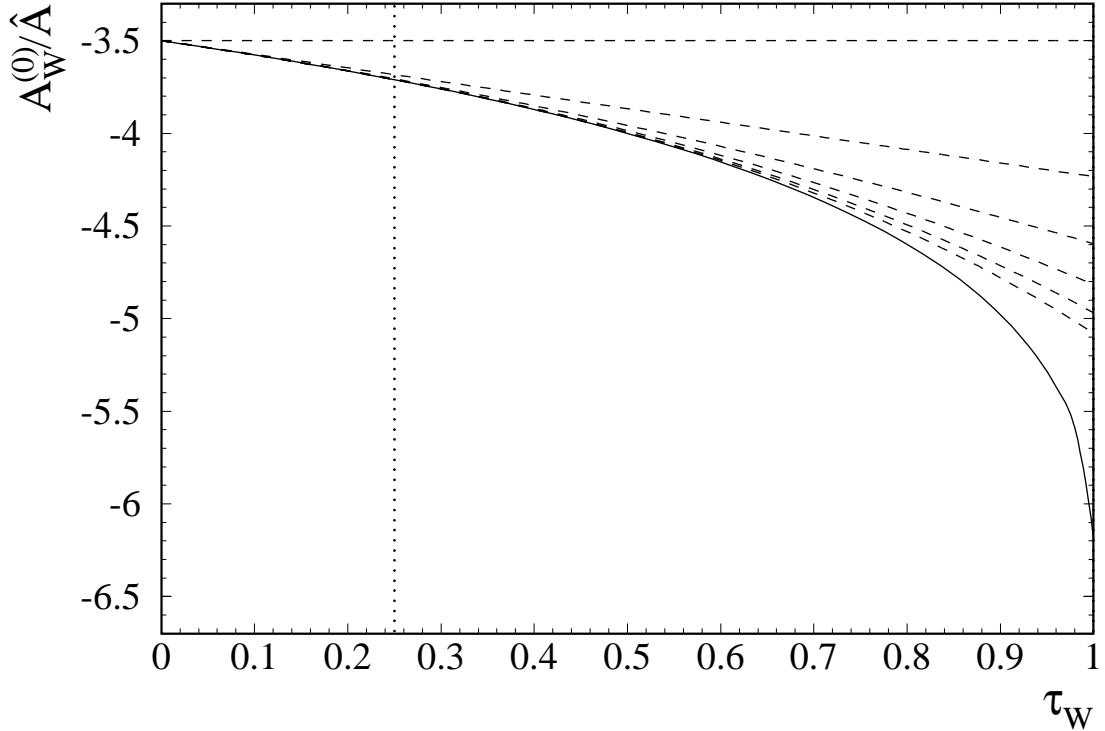


Figure 5: W -boson-induced one-loop amplitude $\mathcal{A}_W^{(0)}$ normalized to \hat{A} as a function of τ_W . The solid curve indicates the exact result, while the dashed curves represent the sequence of approximations that are obtained by successively including higher powers of τ_W in the expansion. The dotted vertical line and the right edge of the frame encompass the intermediate-mass range of the Higgs boson.

5 Conclusions

We calculated the dominant two-loop electroweak correction, of $\mathcal{O}(G_F M_t^2)$, to the partial width of the decay into two photons of the SM Higgs boson in the intermediate mass range, $M_W \leq M_H \leq 2M_W$, where this process is of great phenomenological relevance for the searches at hadron colliders of this elusive missing link of the SM.

We evaluated the relevant Feynman diagrams by application of the asymptotic-expansion technique exploiting the mass hierarchy $2M_t \gg 2M_W \gg M_H$. In this way, we obtained an expansion of the full $\mathcal{O}(G_F M_t^2)$ result in the mass ratio $\tau_W = M_H^2/(2M_W)^2$ through $\mathcal{O}(\tau_W^4)$.

The convergence property of this expansion and our experience with the analogue expansion at the Born level, where the exact result is available for reference, lead us to believe that these five terms should provide a very good approximation to the exact

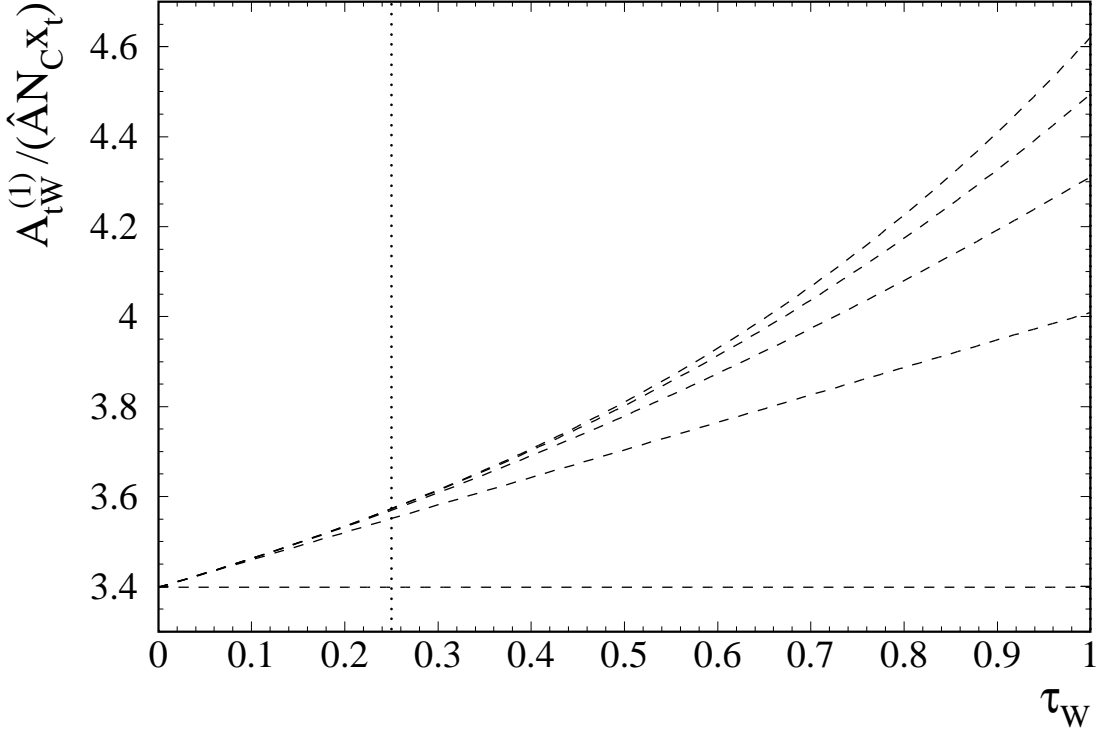


Figure 6: Top-quark-induced two-loop electroweak amplitude $\mathcal{A}_{tW}^{(1)}$ normalized to $\hat{\mathcal{A}}N_c x_t$ as a function of τ_W . The dashed curves represent the sequence of approximations that are obtained by successively including higher powers of τ_W in the expansion. The dotted vertical line and the right edge of the frame encompass the intermediate-mass range of the Higgs boson.

result for $M_H \lesssim 140$ GeV. By the same token, the deviation of this approximation for the $\mathcal{O}(G_F M_t^2)$ amplitude $\mathcal{A}_{tW}^{(1)}$ from the unknown exact result for this quantity is likely to range from 2% to 20% as the value of M_H runs from 140 GeV to $2M_W$.

In the intermediate Higgs-boson mass range, the $\mathcal{O}(G_F M_t^2)$ electroweak correction reduces the size of $\Gamma(H \rightarrow \gamma\gamma)$ by approximately 2.5% and thus fully cancels the positive shift due to the well-known $\mathcal{O}(\alpha_s)$ QCD correction [4].

As a by-product of our analysis, we also recovered the $\mathcal{O}(G_F M_t^2)$ correction to the partial width of the decay into two gluon jets of the intermediate-mass Higgs boson, in agreement with the literature [19].

Acknowledgements

We thank Paolo Gambino for a useful communication. This work was supported in part by the Bundesministerium für Bildung und Forschung through Grant No. 05 HT4GUA/4,

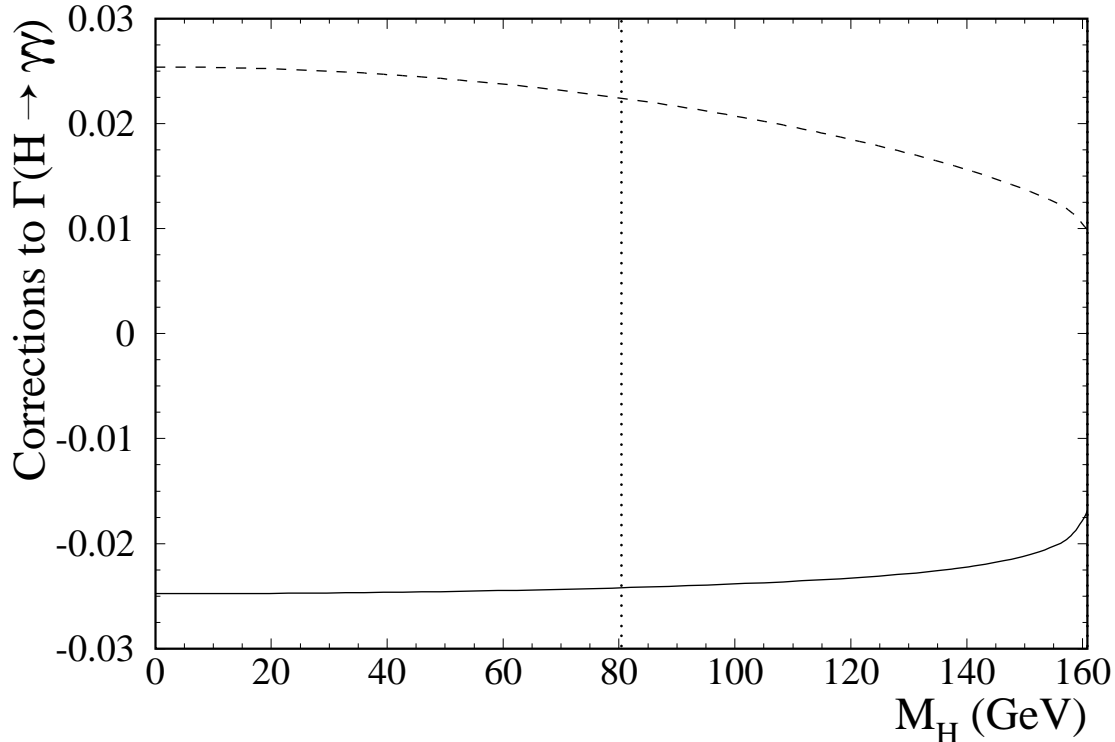


Figure 7: Dominant two-loop corrections to $\Gamma(H \rightarrow \gamma\gamma)$ as functions of M_H . The $\mathcal{O}(G_F M_t^2)$ electroweak correction (solid curve) is compared with the $\mathcal{O}(\alpha_s)$ QCD one (dashed curve). The dotted vertical line and the right edge of the frame encompass the intermediate-mass range of the Higgs boson.

by the Deutsche Forschungsgemeinschaft through Grant No. KN 365/1-1, by the Helmholtz-Gemeinschaft Deutscher Forschungszentren through Grant No. VH-NG-008, and by Sun Microsystems through Academic Equipment Grant No. EDUD-7832-000332-GER.

References

- [1] The LEP Collaborations ALEPH, DELPHI, L3, OPAL, the LEP Electroweak Working Group, the SLD Electroweak and Heavy Flavour Groups, D. Abbaneo et al., Report No. CERN-EP/2003-091, hep-ex/0312023.
- [2] J.R. Ellis, M.K. Gaillard, D.V. Nanopoulos, Nucl. Phys. B 106 (1976) 292; B.L. Ioffe, V.A. Khoze, Fiz. Elem. Chastits At. Yadra 9 (1978) 118, [Sov. J. Part. Nucl. 9 (1978) 50].

- [3] B.A. Kniehl, *Phys. Rept.* 240 (1994) 211;
M. Spira, *Fortsch. Phys.* 46 (1998) 203.
- [4] H. Zheng, D. Wu, *Phys. Rev. D* 42 (1990) 3760;
A. Djouadi, M. Spira, J.J. van der Bij, P.M. Zerwas, *Phys. Lett. B* 257 (1991) 187;
S. Dawson, R.P. Kauffman, *Phys. Rev. D* 47 (1993) 1264;
A. Djouadi, M. Spira, P.M. Zerwas, *Phys. Lett. B* 311 (1993) 255;
K. Melnikov, O.I. Yakovlev, *Phys. Lett. B* 312 (1993) 179;
M. Inoue, R. Najima, T. Oka, J. Saito, *Mod. Phys. Lett. A* 9 (1994) 1189;
J. Fleischer, O.V. Tarasov, *Z. Phys. C* 64 (1994) 413;
J. Fleischer, O.V. Tarasov, V.O. Tarasov, *Phys. Lett. B* 584 (2004) 294.
- [5] M. Steinhauser, in: B.A. Kniehl (Ed.), *Proceedings of the Ringberg Workshop on the Higgs Puzzle — What can we learn from LEP2, LHC, NLC, and FMC?*, Ringberg Castle, Germany, 8–13 December 1996, World Scientific, Singapore, 1997, p. 177, Report No. hep-ph/9612395.
- [6] U. Aglietti, R. Bonciani, G. Degrassi, A. Vicini, Report No. Rome1-1373/04, Freiburg-THEP 04/05, RM3-TH/04-6, IFUM-788/FT, hep-ph/0404071.
- [7] V.A. Smirnov, *Applied Asymptotic Expansions in Momenta and Masses*, Springer-Verlag, Berlin-Heidelberg, 2001.
- [8] Particle Data Group, K. Hagiwara et al., *Phys. Rev. D* 66 (2002) 010001.
- [9] P. Nogueira, *J. Comput. Phys.* 105 (1993) 279.
- [10] T. Seidensticker, unpublished.
- [11] T. Seidensticker, in: G. Athanasiou (Ed.), *Proceedings of the 6th International Workshop on New Computing Techniques in Physics Research: Software Engineering, Artificial Intelligence, Neural Nets, Genetic Algorithms, Symbolic Algebra, Automatic Calculation (AIHENP'99)*, Heraklion, Greece, 12–16 April 1999, SPIRES Conference No C99/04/12, Report No. hep-ph/9905298;
R. Harlander, T. Seidensticker, M. Steinhauser, *Phys. Lett. B* 426 (1998) 125.
- [12] M. Steinhauser, *Comput. Phys. Commun.* 134 (2001) 335.
- [13] J.A.M. Vermaasen, *Symbolic Manipulation with FORM*, Computer Algebra Netherlands, Amsterdam, 1991.
- [14] A.I. Vainshtein, M.B. Voloshin, V.I. Zakharov, M.A. Shifman, *Yad. Fiz.* 30 (1979) 1368 [*Sov. J. Nucl. Phys.* 30 (1979) 711].
- [15] B.A. Kniehl, A. Sirlin, *Phys. Lett. B* 318 (1993) 367;
B.A. Kniehl, *Phys. Rev. D* 50 (1994) 3314.

- [16] Y. Liao, X. Li, Phys. Lett. B 396 (1997) 225.
- [17] A. Djouadi, P. Gambino, B.A. Kniehl, Nucl. Phys. B 523 (1998) 17.
- [18] B.A. Kniehl, M. Spira, Z. Phys. C 69 (1995) 77;
W. Kilian, Z. Phys. C 69 (1995) 89;
K.G. Chetyrkin, B.A. Kniehl, M. Steinhauser, Nucl. Phys. B 510 (1998) 61.
- [19] A. Djouadi, P. Gambino, Phys. Rev. Lett. 73 (1994) 2528;
K.G. Chetyrkin, B.A. Kniehl, M. Steinhauser, Phys. Rev. Lett. 78 (1997) 594;
K.G. Chetyrkin, B.A. Kniehl, M. Steinhauser, Nucl. Phys. B 490 (1997) 19.